

Redox Conditions Affect Ultrafast Exciton Transport in Photosynthetic Pigment–Protein Complexes

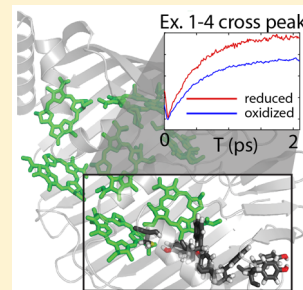
Marco A. Allodi,^{†,‡,§,¶} John P. Otto,^{†,‡} Sara H. Sohail,[†] Rafael G. Saer,^{‡,§,¶} Ryan E. Wood,[†] Brian S. Rolczynski,[†] Sara C. Massey,^{†,¶} Po-Chieh Ting,[†] Robert E. Blankenship,^{‡,§,¶} and Gregory S. Engel^{*,†,¶}

[†]Department of Chemistry, The Institute for Biophysical Dynamics, The James Franck Institute, The University of Chicago, Chicago, Illinois 60637, United States

[‡]Department of Chemistry, [§]Department of Biology, and [¶]The Photosynthetic Antenna Research Center, Washington University in St. Louis, St. Louis, Missouri 63130, United States

Supporting Information

ABSTRACT: Pigment–protein complexes in photosynthetic antennae can suffer oxidative damage from reactive oxygen species generated during solar light harvesting. How the redox environment of a pigment–protein complex affects energy transport on the ultrafast light-harvesting time scale remains poorly understood. Using two-dimensional electronic spectroscopy, we observe differences in femtosecond energy-transfer processes in the Fenna–Matthews–Olson (FMO) antenna complex under different redox conditions. We attribute these differences in the ultrafast dynamics to changes to the system–bath coupling around specific chromophores, and we identify a highly conserved tyrosine/tryptophan chain near the chromophores showing the largest changes. We discuss how the mechanism of tyrosine/tryptophan chain oxidation may contribute to these differences in ultrafast dynamics that can moderate energy transfer to downstream complexes where reactive oxygen species are formed. These results highlight the importance of redox conditions on the ultrafast transport of energy in photosynthesis. Tailoring the redox environment may enable energy transport engineering in synthetic light-harvesting systems.



Pigment–protein complexes enable the primary steps of photosynthesis, from absorption to charge separation.^{1,2} In the green sulfur bacterium (GSB) *Chlorobaculum tepidum*, the tightly packed chromophores in the Fenna–Matthews–Olson (FMO) complex act as an energetic funnel, transferring light energy from the chlorosome to the organism's type I reaction center via exciton energy transfer (EET).^{3–9} Molecular excited states can also supply energy to generate reactive oxygen species (ROS) from molecular oxygen.¹⁰ For example, in GSB, ferredoxin reduced by the reaction center reacts readily with molecular oxygen to produce superoxide.¹¹

Photosynthetic organisms have evolved protective mechanisms to quench excess excitations to prevent ROS formation.^{12,13} Recent work has shown that excitations in the FMO complex are affected by redox conditions,¹⁴ generating questions on what, if any, role FMO may play in protecting GSB from oxidative damage. Strong reducing agents, such as sodium dithionite, have long been known to increase the fluorescence yield of FMO.^{15,16} Point mutations replacing two cysteine residues with alanine eliminated this “dithionite effect”, suggesting a quenching mechanism that utilizes thyl radical on oxidized cysteines.¹⁴ The mutated residues Cys353 and Cys49 are 4.9 Å away from chromophores composing some of the lowest-energy excitons,¹⁷ making them well positioned to quench excitations in the FMO complex before they transfer from bacteriochlorophyll site III into the reaction center.

In contrast to the approach taken by photosynthetic organisms to quench excitations before they generate ROS, enzymes that perform redox chemistry in the presence of oxygen have mechanisms to protect the active site of the protein from being damaged after the formation of ROS. Many enzymes have a set of redox-accessible sulfur-containing amino acids, such as cysteine or methionine, near the active site,¹⁸ and recent work has also found a complementary mechanism in which a tyrosine/tryptophan (Tyr/Trp) chain several residues long can transport the hole created by oxidation out to the solvent-exposed region of the protein, where it can be reduced by radical scavengers.^{19–22} In these enzymes, this structural moiety provides additional protection to the parts of a protein particularly susceptible to damage from ROS.

In this work, we investigate how the oxidative state of amino acid side chains in the vicinity of chromophore molecules affects the system–bath coupling and therefore also ultrafast energy transfer through a pigment–protein complex. We perform two-dimensional electronic spectroscopy (2DES^{23–25}) measurements on both wild-type complexes and mutant complexes lacking cysteine residues under different redox conditions. The cysteine-mediated mechanism proposed

Received: October 30, 2017

Accepted: December 13, 2017

Published: December 13, 2017

by Orf et al.¹⁴ quenches excitations on long time scales under oxidizing conditions. Surprisingly, we also find clear differences in the dynamics under different redox conditions in cysteine-lacking C353A/C49A FMO mutants. Because 2DES allows us to observe directly which excitons are affected by redox conditions, we identify that some residues other than cysteine near sites III and IV must change their redox state to affect EET through the FMO complex on the femtosecond (10^{-15} s) time scale. We identify a Tyr/Trp chain as a structural moiety in the vicinity of sites III and IV that is likely redox-sensitive. Oxidation of these residues could affect energy transfer. The FMO complex is a common model system for exciton energy transfer in photosynthetic pigment–protein complexes. We now observe differences in ultrafast energy transfer as a function of redox conditions on the time scales of the initial photosynthetic light-harvesting event.

We performed 2DES measurements at 77 K under two different experimental conditions. In one set of experiments, FMO complexes were handled under ambient atmospheric conditions, which we refer to as oxidative conditions, as previous literature studies have done.¹⁴ In the other set, sodium dithionite was added to a mixture of protein, glycerol, and buffer to a dithionite concentration of 10 mmol before vitrification. The structure of the FMO complex and the linear absorption spectra of the different samples can be seen in Figure 1. Sodium dithionite is a strong reducing agent ($E^{\circ'} =$

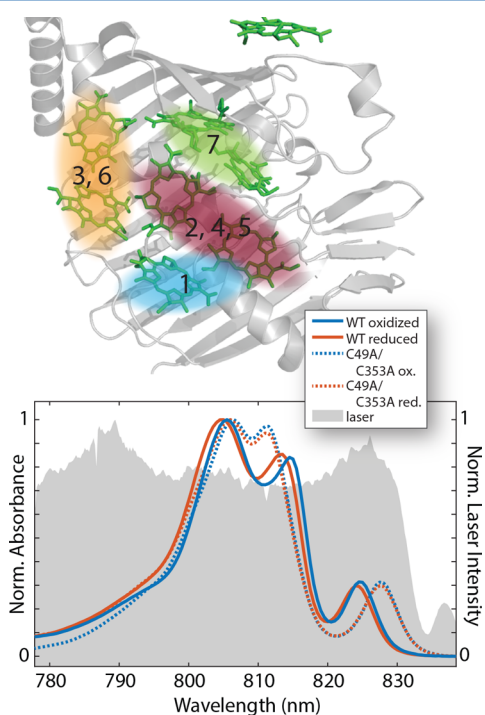


Figure 1. (top) Structure of the FMO complex with excitons labeled with Arabic numerals. The bacteriochlorophyll molecules are colored green, and the positions of the excitons are shown in shaded color. The contribution of different bacteriochlorophyll molecules was taken from Cho et al.²⁶ The FMO structure is taken from PDB 3ENI.²⁷ (bottom) Absorption spectra of samples and the laser bandwidth. Solid blue lines show oxidized wild-type FMO, solid red show reduced wild-type FMO, and dotted blue and red lines show oxidized and reduced C49A/C353A mutant FMO, respectively. The laser intensity as measured on the same instrument as the 2D data is shown in gray. All absorption spectra are measured at 77 K.

-1.07 V vs NHE at pH 10.5²⁸) that reacts with molecular oxygen, effectively removing it from solution. To provide statistically significant measurements of our error, the 2DES data presented are averages of 25 independent 2DES measurements taken on a GRAPES spectrometer.^{29–31} All data presented are normalized to the maximum of the spectrum at zero waiting time ($T = 0$). Additional information about the experimental methods can be found in the Supporting Information. The correlations between excitation and detection wavelength for wild-type FMO under oxidative or reductive conditions are shown in Figure 2A–D.

Because the below-diagonal cross-peak amplitudes result from downhill energy transfer, we compare the intensity of these features under the oxidative and reducing conditions. One major pathway through the FMO complex involves energy transport from exciton 7 to exciton 4, through exciton 2, and finally into exciton 1.^{26,32,33} This pathway shows redox-environment-dependent differences in ultrafast dynamics and efficiency of energy transfer. Under oxidized or reduced conditions, the traces in Figure 2F, which are taken at the 4–2 cross peak, show differences in both normalized amplitude and dynamics between the reduced and oxidized experiments. The panels in Figure 2H,I show energy-transfer cross peaks into exciton 1, demonstrating clear differences in the transport dynamics through the FMO complex. When we fit an exponential decay starting at the peak value of the 4–2 cross peak, this cross peak decays with a 710 fs time constant in the reduced experiment, compared with a 1300 fs time constant in the oxidized experiment. The 4–1 cross peak in the reduced data grows in faster (460 fs reduced vs 492 fs oxidized) and also reaches a larger amplitude (almost 1, Figure 2I). All fits can be found in Table ST2. We conclude from these data that the different oxidative conditions affect the energy flow into and out of excitons 2 and 4, which are known to be associated with chromophores at sites III and IV.²⁶

Looking at the diagonal peak traces, which report on exciton populations, we see evidence that a trap or quenching site affects the ultrafast dynamics. The exciton 4 energy traces, shown in Figure 2E, exhibit different dynamics in waiting time; both traces start from similar initial normalized amplitudes, and the excitation in the oxidized experiment decays slightly more quickly than the reduced case. Also, the exciton 2 diagonal features (Figure 2G) show the same, but more pronounced, trend as the exciton 4 diagonal features. Some trap or quenching site must be removing excitations faster in the oxidized versus the reduced experiment. The cysteine-mediated quenching certainly contributes to these dynamics, and we confirm that the cysteine-mediated mechanism is still in effect by collecting 2DES spectra at different waiting times between 5 ps and 1 ns. We observe trends in these picosecond dynamics consistent with the previous work by Orf et al.; see Figure S3.¹⁴

The interactions between the pigments and the protein in the FMO complex determine both the static electronic structure and the dynamics. The protein acts as a scaffold that holds the chromophores in a fixed position and orientation, thus defining the site energies and coupling that generate the electronic system Hamiltonian. Vibrational motions within the protein serve as a bath that couples to the chromophores, giving rise to the spectral density. Quantum mechanically, energy transfer between excitonic states must be driven by coupling between the system and the bath.^{34–36} As a result, changes to the local electrodynamic environment affect transport through the FMO complex.

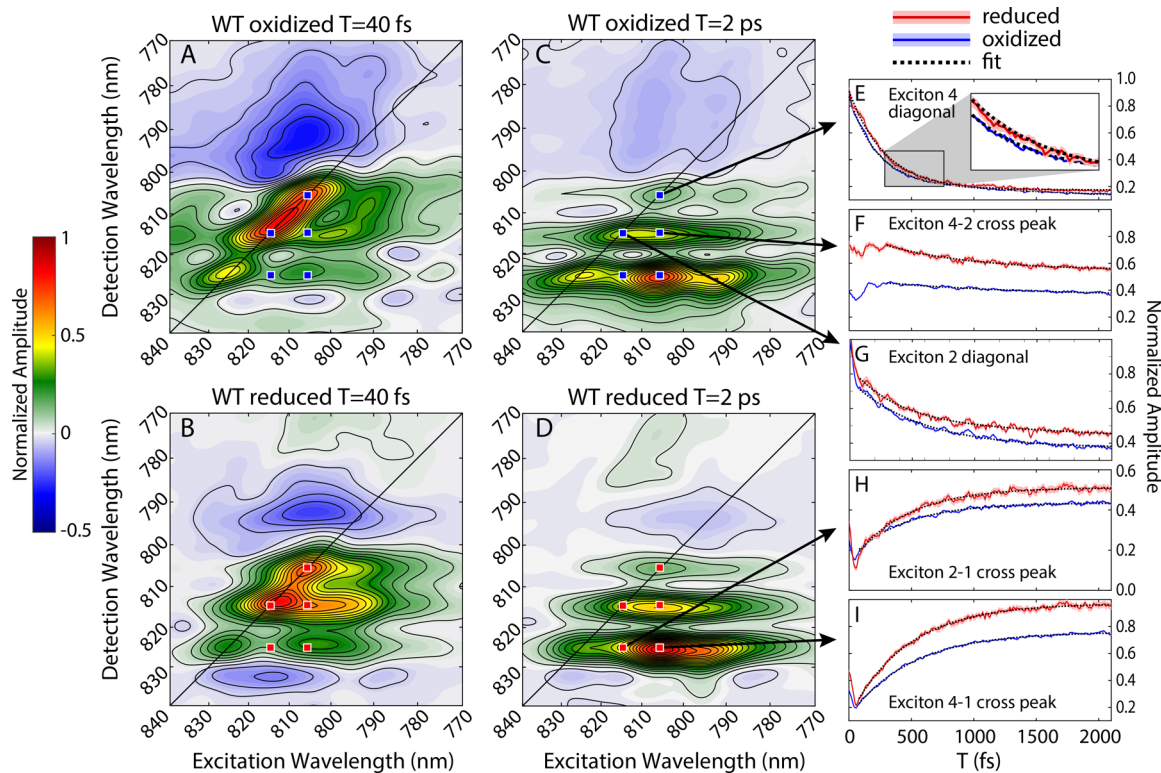


Figure 2. Two-dimensional electronic spectra of wild-type FMO showing redox-dependent ultrafast dynamics. (A,B) 2D spectra of FMO at early waiting times. (C,D) 2D spectra at longer waiting times. (E–I) Representative time traces taken at the spots indicated by blue (oxidized) or red (reduced) markers. The dotted black lines shown with the traces were obtained by a least-squares fit to the data. The shading around the colored lines represents the standard error of the mean from 25 independent measurements. The inset in E allows a clear view of the error bars.

Differences in EET can result from differences in the coupling of the chromophore system to the protein–bath environment or from differences in the chromophores' positions and orientation with respect to each other, thus changing the system Hamiltonian. Changes to the system result in changes to the exciton peak positions. Small differences can be seen in the linear spectra under oxidizing vs reducing conditions in Figure 1. Because the shifts in the linear spectra are small, we focus our discussion on differences in system–bath coupling.

An analysis of the absorptive 2D line shape of the FMO complex provides direct evidence for differences in the system–bath coupling because the time evolution of the line shape is a direct reporter of the bath spectral densities that modulate the energy of the surrounding excitons.³⁷ As seen in Figure 2A–D, the positive diagonal features at around 825, 812, and 805 nm correspond to the energies of excitons 1, 2, and 4, respectively.^{26,33} These positive peaks along the diagonal in both the oxidized and reduced data sets show diagonal elongation at early times corresponding to an inhomogeneous environment surrounding the chromophores.

The spectral diffusion can be quantified using a centerline slope analysis.³⁸ In the reduced experiments, this diagonal elongation rapidly disappears; the exciton 1 feature at 825 nm has a decay of the centerline slope of 30 fs, while the exciton 4 feature at 805 nm can be fit with a 160 fs time constant. Plots of the centerline slope can be seen in Figure 3. In contrast, the inhomogeneous broadening is larger in the oxidized experiments at early times and persists over all time scales measured in these experiments.

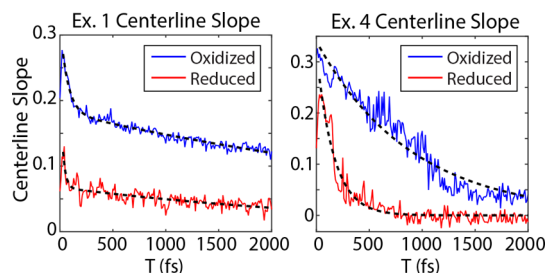


Figure 3. Centerline slope decay for two different excitons in wild-type FMO. Higher slopes indicate greater inhomogeneous contribution to the feature line shape.

The differences in inhomogeneous broadening shows that oxidative conditions change the local environment around excitons 4, 2, and 1 and affect the system–bath coupling. Under reducing conditions, spectral diffusion produces round line shapes as the bath effectively solvates the excited-state charge distribution.³⁹ In contrast, under oxidative conditions, a set of different charge distributions around these chromophores produces the inhomogeneous line shape observed in Figure 2C,D. As such, changes caused by oxidation of the residues around excitons 4, 2, and 1 change the spectral densities of the bath, and this spectral density appears not to solvate the excited-state electron distribution as effectively as under reductive conditions. In addition, because the centerline slope analysis shows that spectral diffusion happens slightly faster at higher-energy excitons in the reduced wild type, we know that the bath is not the same around each exciton. These tailored, different spectral densities likely play a key role in controlling energy transfer through the complex, and further investigation

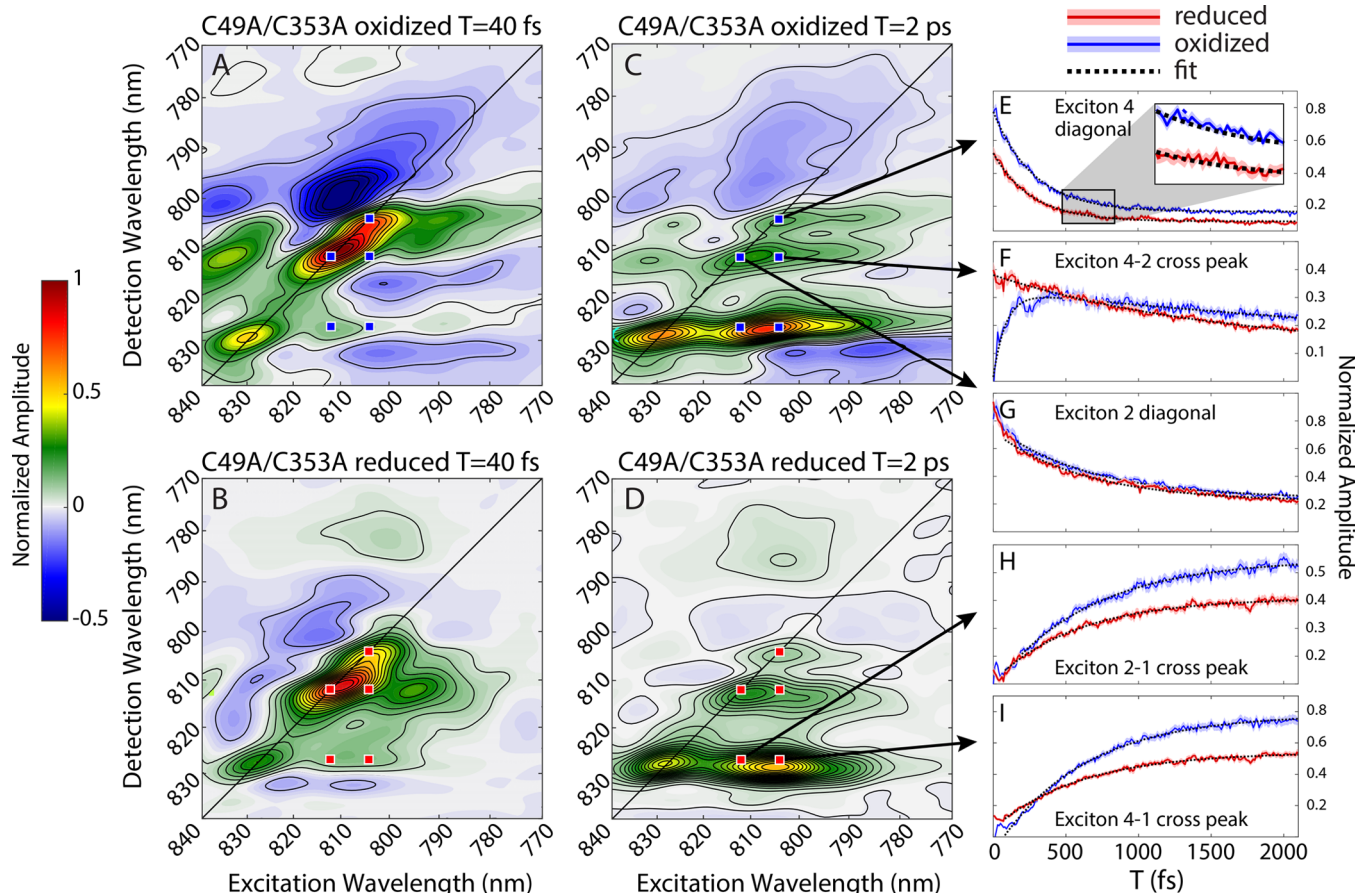


Figure 4. Two-dimensional electronic spectra of mutant C49A/C353A FMO showing redox-dependent ultrafast dynamics. (A,B) 2D spectra at early waiting times. (C,D) 2D spectra at longer waiting times. (E–I) Representative time traces taken at the spots indicated by blue (oxidized) or red (reduced) markers. The dotted black lines shown with the traces are a least-squares fit to the data. The shading around the colored lines represents the standard error of the mean from 25 independent measurements. The inset in E allows a clear view of the error bars.

is necessary to understand the role that these differences may play. This mechanism has implications for modeling exciton transport as recent theoretical work has calculated differences in spectral densities around different chromophores.⁴⁰

To understand if the effects of different redox conditions on EET are related to, or distinct from, the cysteine-mediated mechanism previously discovered in FMO, we performed 2DES measurements on the mutant FMO strain C49A/C353A. If the cysteine-mediated mechanism were the only redox-dependent mechanism that affected EET in the FMO complex, eliminating these cysteines should remove the differences in the dynamics observed in the 2DES measurements of the wild type. However, a comparison between mutant and wild-type 2DES measurements shows that the redox-active cysteines alone cannot be responsible for the differences observed in the wild-type spectra.

The redox-dependent differences in the dynamics of the mutant complexes are even larger than those of the wild-type complexes. 2DES spectra are presented in Figure 4A–D. Figure 4E shows that, in the mutant, the decay of the exciton 4 diagonal peak displays different relative amplitudes and time constants, depending on the redox condition, while Figure 4G shows that the diagonal peak at exciton 2 displays similar dynamics between the two conditions. As in the wild type, the redox condition affects the dynamics of the 4–2 cross peak in the mutant. While there is still rapid transfer from 4 to 2 followed by decay in the reduced mutant sample, the oxidized

mutant sample shows much slower growth followed by decay. Also, both the 4–1 (Figure 4I) and 2–1 (Figure 4H) cross peaks show different dynamics to the wild type as the signals from oxidized complexes grow in faster than those of the reduced complexes. Finally, both the oxidized and reduced experiment show a more inhomogeneous line shape than that in the wild type, with persistent inhomogeneity out to 2 ps (Figure 4A–D). These line shape differences show that the system–bath coupling has meaningfully changed as a result of these mutations. 2DES measurements at long waiting times confirm that the mutant dynamics at long waiting times is the same, in agreement with Orf et al. (Figure S3).

A set of redox-active residues in the vicinity of excitons 4, 2, and 1 would explain the differences observed in the EET pathways in the wild-type and mutant FMO complexes under different redox conditions. Sulfur-containing amino acids, such as cysteine and methionine, are well-understood components of the redox proteome that manage protein response to oxidative stress.⁴¹ As the cysteine residues at sites 49 and 353 in FMO are the only sulfur-containing residues in close enough proximity to interact with the chromophores and our mutants lack the cysteines, oxidation of other redox-sensitive residues, such as tyrosine or tryptophan, provides another possible explanation for the trends observed in the data. Tryptophan and tyrosine molecules in solution at pH 10.5 can be oxidized at potentials around 0.7 V vs NHE,⁴² and tryptophan and tyrosine residues in proteins are broadly considered susceptible to oxidation at

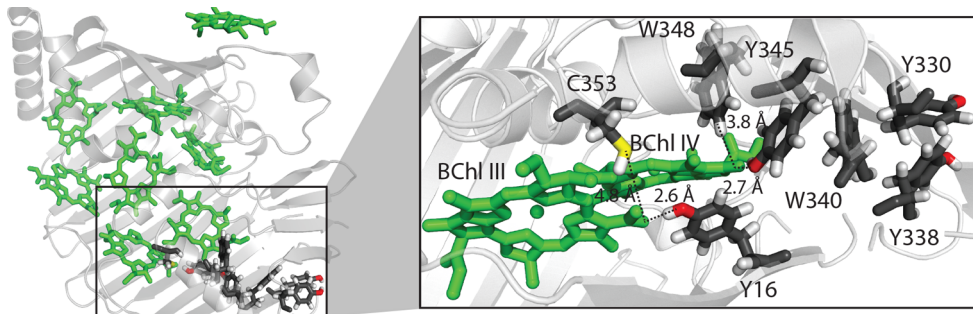


Figure 5. Structure of the FMO complex showing a Tyr/Trp in the vicinity of sites III and IV. The protein backbone is colored gray, while the BChl molecules are colored green with the phytol tails removed for clarity. The residues of interest are labeled and are colored so that C is black, O is red, and S is yellow. Y345, W348, and C353 are collocated on the same α -helix. Coordinates are taken from PDB structure 3ENI.²⁷ The distances reported are heavy-atom distances with hydrogens added.

potentials in the vicinity of 1 V vs NHE,²⁰ within reach of superoxide ions generated by reduced ferredoxin.¹⁰ Previous work has shown electron paramagnetic resonance (EPR) signatures consistent with tyrosine radicals in oxidized FMO.¹⁶

As discussed by Gray and Winkler, Tyr/Trp chains, where one end starts in the interior of the protein and the other is solvent-accessible, are likely to play a role in protecting proteins from oxidative damage.^{20,21} In the FMO complex, there exists only one chain of tyrosine and tryptophan residues facing into the chromophores, and this chain is in the vicinity of BChl sites III and IV, the sites that contribute to excitons 4, 2, and 1. The six residues (Y16, W348, Y345, W340, Y338, and Y330) in the Tyr/Trp chain can be seen in Figure 5. Situated near site III, an oxidized Tyr/Trp chain could prevent excitations from reaching the reaction center. There are six other tryptophan and six other tyrosine residues in the structure. None are in an extended chain, and all but two tryptophan residues (W184 and W239) are completely solvent-exposed or more than 4 Å away from any chromophores.

The presence of a hole along the Tyr/Trp chain will change the electrostatics of these chromophores, thus affecting the system–bath coupling and the transport properties that depend on it.^{18,43} The differences in electronic structure between the mutant and wild-type complexes also contribute to the differences between their EET dynamics. The changes in electronic structure can be clearly seen as shifts in the peak centers and line shape in both the linear absorption spectrum (Figure 1) and the 2DES measurements. In the mutants, because the C353 residue is also in this same pocket as the chain, the absence of the large, polarizable sulfur atom is likely to perturb how the Tyr/Trp chain affects the system–bath coupling. Finally, as Figure 5 clearly shows, C353, W348, and Y345 all are part of the same α -helix. In addition, Y16, W348, Y345, W340, and Y338 residues are highly conserved across 28 different species of GSB⁴⁴ and are as conserved as the C353 residue.¹⁴

There may be other factors that affect the redox-dependent ultrafast dynamics in FMO as well. Two isolated tryptophan residues, W184 and W239, are 3.2 and 3.9 Å away from opposite sides of site VI (Figure S2), the major contributor to exciton 7, meaning that their oxidation could affect the system–bath coupling around that exciton. Groupings of aromatic residues have been understood to help stabilize protein folding and assist ligand binding,^{45–47} and because residue W184 is adjacent to F185, these residues likely play a structural role. In addition, these residues are in the chromophore pocket and not solvent-exposed; therefore, there is no way to transfer the

strongly oxidizing hole away from the chromophores. However, if they are near site VI to help regulate energy transfer in oxidizing conditions, they would be regulating the same major pathway through the FMO complex as the Tyr/Trp chain near site IV. In addition, isolated FMO proteins can form aggregates after being solubilized. Aggregates of other photosynthetic pigment–protein complexes have shown aggregation-dependent quenching based on a charge-transfer mechanism on the nanosecond time scale.^{48,49} However, given the time scales for charge transfer in aggregation-dependent quenching in other complexes, it seems unlikely that this would lead to the significant differences in ultrafast dynamics observed here.

We observe differences in the ultrafast EET in the FMO pigment–protein complex under different redox conditions. We attribute the differences in EET dynamics primarily to differences in the system–bath coupling between BChl chromophores and protein residues. On the basis of recent work by Gray and Winkler,^{20,21} we speculate that the changes in ultrafast EET dynamics are strongly influenced by the redox-active Tyr/Trp chain in the vicinity of two key chromophores that affect the lowest-energy excitons in the system, a mechanism that is distinct from the previously reported cysteine-mediated quenching mechanism. When the residues surrounding the chromophores are oxidized, they change the electronic environment in which the chromophores sit, ultimately affecting EET through the complex. The most efficient and rapid transfer through the excitonic system occurs under reducing conditions free of oxygen, similar to the anaerobic conditions under which FMO operates in nature. While Tyr/Trp chains have been widely studied in enzymes that produce oxidizing intermediates during catalysis, more work needs to be done to understand the role they may play in photosynthetic pigment–protein complexes. Additionally, a redox-sensitive environment may ultimately provide a useful handle for controlling EET in artificial/synthetic systems for light harvesting and solar-energy conversion.

■ ASSOCIATED CONTENT

§ Supporting Information

The Supporting Information is available free of charge on the ACS Publications website at DOI: [10.1021/acs.jpclett.7b02883](https://doi.org/10.1021/acs.jpclett.7b02883).

Experimental methods, additional 2DES spectra at different waiting times, protein structure around BChl VI, integrated 2DES data for comparison with picosecond pump–probe measurements, absolute value time

traces, real-valued time traces at different exciton positions, and tables of exponential fit parameters (PDF)

AUTHOR INFORMATION

Corresponding Author

*E-mail: gsengel@uchicago.edu.

ORCID

Marco A. Allodi: 0000-0002-3289-1659

Sara C. Massey: 0000-0002-1602-3325

Gregory S. Engel: 0000-0002-6740-5243

Author Contributions

#M.A.A. and J.P.O. contributed equally to this work.

Notes

The authors declare no competing financial interest.

ACKNOWLEDGMENTS

This work was supported by the Department of Defense as part of the Vannevar Bush Fellowship (N00014-15-1-0048 and N00014-16-1-2513), the Air Force Office of Scientific Research (FA9550-14-1-0367), and the Dreyfus Foundation. Additional support was provided by the Chicago MRSEC, which is funded by the NSF through Grant DMR-1420709. M.A.A. acknowledges support from an Arnold O. Beckman Postdoctoral Fellowship from the Arnold and Mabel Beckman Foundation and from a Yen Postdoctoral fellowship from the Institute for Biophysical Dynamics at The University of Chicago. S.H.S, R.E.W, and S.C.M were each supported individually by a National Defense Science and Engineering Graduate (NDSEG) Fellowship, 32 CFR 168a. R.E.B and R.G.S acknowledge funding from the Photosynthetic Antenna Research Center, an Energy Frontier Research Center funded by the U.S. Department of Energy, Office of Science, Office of Basic Energy Sciences, under Award DE-SC 0001035.

REFERENCES

- Clayton, R. K.; Clayton, B. J. B850 pigment-protein complex of *Rhodopseudomonas sphaeroides*: Extinction coefficients, circular dichroism, and the reversible binding of bacteriochlorophyll. *Proc. Natl. Acad. Sci. U. S. A.* **1981**, *78* (9), 5583–5587.
- Liu, Z.; Yan, H.; Wang, K.; Kuang, T.; Zhang, J.; Gui, L.; An, X.; Chang, W. Crystal structure of spinach major light-harvesting complex at 2.72 Å resolution. *Nature* **2004**, *428* (6980), 287–292.
- Wahlund, T. M.; Woese, C. R.; Castenholz, R. W.; Madigan, M. T. A thermophilic green sulfur bacterium from New Zealand hot springs, *Chlorobium tepidum* sp. nov. *Arch. Microbiol.* **1991**, *156* (2), 81–90.
- Blankenship, R. E. *Molecular mechanisms of photosynthesis*, 2nd ed.; Wiley/Blackwell: Chichester, West Sussex, 2014; p xv-296.
- Fenna, R.; Matthews, B. Chlorophyll arrangement in a bacteriochlorophyll protein from *Chlorobium limicola*. *Nature* **1975**, *258*, 573–577.
- Zhang, W. M.; Meier, T.; Chernyak, V.; Mukamel, S. Exciton-migration and three-pulse femtosecond optical spectroscopies of photosynthetic antenna complexes. *J. Chem. Phys.* **1998**, *108* (18), 7763–7774.
- Hayes, D.; Panitchayangkoon, G.; Fransted, K. A.; Caram, J. R.; Wen, J.; Freed, K. F.; Engel, G. S. Dynamics of electronic dephasing in the Fenna-Matthews-Olson complex. *New J. Phys.* **2010**, *12* (6), 065042.
- Hayes, D.; Engel, G. S. Extracting the Excitonic Hamiltonian of the Fenna-Matthews-Olson Complex Using Three-Dimensional Third-Order Electronic Spectroscopy. *Biophys. J.* **2011**, *100* (8), 2043–2052.
- Dostál, J.; Pšenčík, J.; Zigmantas, D. In situ mapping of the energy flow through the entire photosynthetic apparatus. *Nat. Chem.* **2016**, *8*, 705.
- Krumova, K.; Cosa, G., Overview of Reactive Oxygen Species. In *Singlet Oxygen: Applications in Biosciences and Nanosciences*; Nonell, S., Flors, C., Eds.; Royal Society of Chemistry, 2016; Vol. 1, pp 3–21.
- Orme-Johnson, W. H.; Beinert, H. On the formation of the superoxide anion radical during the reaction of reduced iron-sulfur proteins with oxygen. *Biochem. Biophys. Res. Commun.* **1969**, *36* (6), 905–911.
- Demming-Adams, B.; Garab, B.; Adams, W. W., III; Govindjee, Eds. *Non-Photochemical Quenching and Energy Dissipation in Plants, Algae and Cyanobacteria*; Springer: The Netherlands, 2014; p xxxviii-649.
- Pascal, A. A.; Liu, Z.; Broess, K.; van Oort, B.; van Amerongen, H.; Wang, C.; Horton, P.; Robert, B.; Chang, W.; Ruban, A. Molecular basis of photoprotection and control of photosynthetic light-harvesting. *Nature* **2005**, *436* (7047), 134–137.
- Orf, G. S.; Saer, R. G.; Niedzwiedzki, D. M.; Zhang, H.; McIntosh, C. L.; Schultz, J. W.; Mirica, L. M.; Blankenship, R. E. Evidence for a cysteine-mediated mechanism of excitation energy regulation in a photosynthetic antenna complex. *Proc. Natl. Acad. Sci. U. S. A.* **2016**, *113* (31), E4486–93.
- Karapetyan, N. V.; Swarthoff, T.; Rijgersberg, C. P.; Amesz, J. Fluorescence emission spectra of cells and subcellular preparations of a green photosynthetic bacterium. Effects of dithionite on the intensity of the emission bands. *Biochim. Biophys. Acta, Bioenerg.* **1980**, *593* (2), 254–260.
- Zhou, W.; LoBrutto, R.; Lin, S.; Blankenship, R. E. Redox effects on the bacteriochlorophyll α -containing Fenna-Matthews-Olson protein from *Chlorobium tepidum*. *Photosynth. Res.* **1994**, *41* (1), 89–96.
- Saer, R.; Orf, G. S.; Lu, X.; Zhang, H.; Cuneo, M. J.; Myles, D. A.; Blankenship, R. E. Perturbation of bacteriochlorophyll molecules in Fenna-Matthews-Olson protein complexes through mutagenesis of cysteine residues. *Biochim. Biophys. Acta, Bioenerg.* **2016**, *1857* (9), 1455–1463.
- Go, Y.-M.; Jones, D. P. The Redox Proteome. *J. Biol. Chem.* **2013**, *288* (37), 26512–26520.
- Brettel, K.; Aubert, C.; Vos, M. H.; Mathis, P.; Eker, A. P. M. Intraprotein radical transfer during photoactivation of DNA photolyase. *Nature* **2000**, *405* (6786), 586–590.
- Gray, H. B.; Winkler, J. R. Hole hopping through tyrosine/tryptophan chains protects proteins from oxidative damage. *Proc. Natl. Acad. Sci. U. S. A.* **2015**, *112* (35), 10920–10925.
- Gray, H. B.; Winkler, J. R. The Rise of Radicals in Bioinorganic Chemistry. *Isr. J. Chem.* **2016**, *56* (9–10), 640–648.
- Shih, C.; Museth, A. K.; Abrahamsson, M.; Blanco-Rodriguez, A. M.; Di Bilio, A. J.; Sudhamsu, J.; Crane, B. R.; Ronayne, K. L.; Towrie, M.; Vlcek, A., Jr.; Richards, J. H.; Winkler, J. R.; Gray, H. B. Tryptophan-accelerated electron flow through proteins. *Science* **2008**, *320* (5884), 1760–2.
- Jonas, D. M. Two-dimensional femtosecond spectroscopy. *Annu. Rev. Phys. Chem.* **2003**, *54*, 425–63.
- Mukamel, S. Multidimensional Femtosecond Correlation Spectroscopies of Electronic and Vibrational Excitations. *Annu. Rev. Phys. Chem.* **2000**, *51* (1), 691–729.
- Hybl, J. D.; Albrecht, A. W.; Gallagher Faeder, S. M.; Jonas, D. M. Two-dimensional electronic spectroscopy. *Chem. Phys. Lett.* **1998**, *297* (3), 307–313.
- Cho, M.; Vaswani, H. M.; Brixner, T.; Stenger, J.; Fleming, G. R. Exciton Analysis in 2D Electronic Spectroscopy. *J. Phys. Chem. B* **2005**, *109* (21), 10542–10556.
- Wen, J.; Zhang, H.; Gross, M. L.; Blankenship, R. E. Membrane orientation of the FMO antenna protein from *Chlorobaculum tepidum* as determined by mass spectrometry-based footprinting. *Proc. Natl. Acad. Sci. U. S. A.* **2009**, *106* (15), 6134–6139.

- (28) Mayhew, S. G. The Redox Potential of Dithionite and SO₂ from Equilibrium Reactions with Flavodoxins, Methyl Viologen and Hydrogen plus Hydrogenase. *Eur. J. Biochem.* **1978**, *85* (2), 535–547.
- (29) Harel, E.; Fidler, A. F.; Engel, G. S. Single-Shot Gradient-Assisted Photon Echo Electronic Spectroscopy. *J. Phys. Chem. A* **2011**, *115* (16), 3787–3796.
- (30) Dahlberg, P. D.; Ting, P. C.; Massey, S. C.; Allodi, M. A.; Martin, E. C.; Hunter, C. N.; Engel, G. S. Mapping The Ultrafast Flow of Harvested Solar Energy in Living Photosynthetic Cells. *Nat. Commun.* **2017**, *8*, 988.
- (31) Sohail, S. H.; Dahlberg, P. D.; Allodi, M. A.; Ting, P. C.; Massey, S. C.; Martin, E. C.; Hunter, C. N.; Engel, G. S. Communication: Broad Manifold of Excitonic States in Light-Harvesting Complex 1 Promotes Efficient Unidirectional Energy Transfer. *J. Chem. Phys.* **2017**, *147*, 131101.
- (32) Brixner, T.; Stenger, J.; Vaswani, H. M.; Cho, M.; Blankenship, R. E.; Fleming, G. R. Two-dimensional spectroscopy of electronic couplings in photosynthesis. *Nature* **2005**, *434* (7033), 625–628.
- (33) Thyrhaug, E.; Žídek, K.; Dostál, J.; Bína, D.; Zigmantas, D. Exciton Structure and Energy Transfer in the Fenna–Matthews–Olson Complex. *J. Phys. Chem. Lett.* **2016**, *7* (9), 1653–1660.
- (34) Shankar, R. *Principles of quantum mechanics*; Springer Science & Business Media, 2012; p xviii-676.
- (35) Mukamel, S. *Principles of nonlinear optical spectroscopy*; Oxford University Press: New York, 1995; p xviii-543.
- (36) Lloyd, S.; Chiloyan, V.; Hu, Y.; Huberman, S.; Liu, Z.-W.; Chen, G., No energy transport without discord. *arXiv:1510.05035.2015*.
- (37) Fidler, A. F.; Caram, J. R.; Hayes, D.; Engel, G. S. Towards a coherent picture of excitonic coherence in the Fenna–Matthews–Olson complex. *J. Phys. B: At., Mol. Opt. Phys.* **2012**, *45* (15), 154013.
- (38) Fenn, E. E.; Fayer, M. D. Extracting 2D IR frequency-frequency correlation functions from two component systems. *J. Chem. Phys.* **2011**, *135* (7), 074502.
- (39) Fleming, G. R.; Cho, M. Chromophore-Solvent Dynamics. *Annu. Rev. Phys. Chem.* **1996**, *47* (1), 109–134.
- (40) Lee, M. K.; Coker, D. F. Modeling Electronic-Nuclear Interactions for Excitation Energy Transfer Processes in Light-Harvesting Complexes. *J. Phys. Chem. Lett.* **2016**, *7* (16), 3171–3178.
- (41) Davies, M. J. The oxidative environment and protein damage. *Biochim. Biophys. Acta, Proteins Proteomics* **2005**, *1703* (2), 93–109.
- (42) Tommos, C.; Skalicky, J. J.; Pilloud, D. L.; Wand, A. J.; Dutton, P. L. De Novo Proteins as Models of Radical Enzymes. *Biochemistry* **1999**, *38* (29), 9495–9507.
- (43) Stadtman, E. R.; Levine, R. L. Free radical-mediated oxidation of free amino acids and amino acid residues in proteins. *Amino Acids* **2003**, *25* (3), 207–218.
- (44) Valleau, S.; Studer, R. A.; Häse, F.; Kreisbeck, C.; Saer, R. G.; Blankenship, R. E.; Shakhnovich, E. I.; Aspuru-Guzik, A. Absence of Selection for Quantum Coherence in the Fenna–Matthews–Olson Complex: A Combined Evolutionary and Excitonic Study. *ACS Cent. Sci.* **2017**, *3* (10), 1086–1095.
- (45) Karlin, S.; Bucher, P. Correlation analysis of amino acid usage in protein classes. *Proc. Natl. Acad. Sci. U. S. A.* **1992**, *89* (24), 12165–12169.
- (46) Burley, S.; Petsko, G. Aromatic-aromatic interaction: a mechanism of protein structure stabilization. *Science* **1985**, *229* (4708), 23–28.
- (47) Lanzarotti, E.; Biekofsky, R. R.; Estrin, D. A.; Marti, M. A.; Turjanski, A. G. Aromatic–Aromatic Interactions in Proteins: Beyond the Dimer. *J. Chem. Inf. Model.* **2011**, *51* (7), 1623–1633.
- (48) Ballottari, M.; Girardon, J.; Betterle, N.; Morosinotto, T.; Bassi, R. Identification of the Chromophores Involved in Aggregation-dependent Energy Quenching of the Monomeric Photosystem II Antenna Protein LhcB5. *J. Biol. Chem.* **2010**, *285* (36), 28309–28321.
- (49) Ballottari, M.; Girardon, J.; Dall’Osto, L.; Bassi, R. Evolution and functional properties of photosystem II light harvesting complexes in eukaryotes. *Biochim. Biophys. Acta, Bioenerg.* **2012**, *1817* (1), 143–157.